Lymph node T cell responses predict the efficacy of live attenuated SIV vaccines

Yoshinori Fukazawa[1,*], **Haesun Park**[1,*], **Mark J. Cameron**[2], **Francois Lefebvre**[2], **Richard Lum**[1], **Noel Coombes**[1], **Eisa Mahyari**[1], **Shoko Hagen**[1], **Jin Young Bae**[1], **Marcelo Delos Reyes III**[1], **Tonya Swanson**[1], **Alfred W. Legasse**[1], **Andrew Sylwester**[1], **Scott G. Hansen**[1], **Andrew T. Smith**[2], **Petra Stafova**[2], **Rebecca Shoemaker**[3], **Yuan Li**[3], **Kelli Oswald**[3], **Michael K. Axthelm**[1], **Adrian McDermott**[4], **Guido Ferrari**[5], **David C. Montefiori**[5], **Paul T. Edlefsen**[6], **Michael Piatak Jr.**[3], **Jeffrey D. Lifson**[3], **Rafick P. Sékaly**[2], and **Louis J. Picker**[1]

[1]Vaccine and Gene Therapy Institute, Departments of Molecular Microbiology and Immunology and Pathology, and the Oregon National Primate Research Center, Oregon Health & Science University, Beaverton, OR 97006

[2]Vaccine and Gene Therapy Institute-Florida, Port St. Lucie, FL 34987

[3]AIDS and Cancer Virus Program, SAIC Frederick, Inc., Frederick National Laboratory for Cancer Research, Frederick, MD 21702

[4]Vaccine Research Institute, National Institute of Allergy and Infectious Diseases, Bethesda, MD 20892

[5]Duke University Medical Center, Durham, NC 27710

[6]Statistical Center for HIV/AIDS Research and Prevention, Vaccine and Infectious Disease Division,, Fred Hutchinson Cancer Research Center, Seattle, WA 98109

Abstract

Live attenuated SIV vaccines (LAVs) remain the most efficacious of all vaccines in nonhuman primate (NHP) models of HIV/AIDS, yet the basis of their robust protection remains poorly understood. Here, we demonstrate that the degree of LAV-mediated protection against intravenous wildtype SIVmac239 challenge strongly correlates with the magnitude and function of SIV-specific, effector-differentiated T cells in lymph node, but not with such T cell responses in blood or with other cellular, humoral and innate immune parameters. Maintenance of protective T cell responses was associated with persistent LAV replication in lymph node, which occurred almost

exclusively in follicular helper T cells. Thus, effective LAVs maintain lymphoid tissue-based, effector-differentiated, SIV-specific T cells that intercept and suppress early wildtype SIV amplification and, if present in sufficient frequencies, can completely control and perhaps clear infection, an observation that provides rationale for development of safe, persistent vectors that can elicit and maintain such responses.

INTRODUCTION

It has been two decades since the first report that LAV administration can completely protect rhesus macaques from subsequent challenge with highly pathogenic, wildtype SIV[1], a degree of efficacy that to this day stands in sharp contrast to that achieved with a wide variety of alternative HIV/SIV vaccine strategies[2-6]. Unfortunately, LAV-mediated protection is inversely proportional to the degree of attenuation, such that the most effective designs retain considerable pathogenic potential, precluding their development as vaccines in humans[2,7]. While it has long been appreciated that delineation of a common immunologic mechanism for LAV efficacy would be a major advance for the HIV/AIDS vaccine field – providing an immune response target for development of safe and effective vaccine designs[3] – the basis of LAV efficacy, particularly the durable, complete, apparently sterilizing control characteristic of the best LAVs, remains controversial. Twenty years of research using various types of LAVs and NHP species, as well as different pathogenic challenge viruses and varying timing and routes of challenge has variously implicated, or argued against, T cell immunity, humoral immunity, innate immunity and viral interference in LAV-mediated protection without the emergence of a unifying, consensus protective mechanism, or clear-cut definition of multiple different mechanisms acting in combination to achieve protection [2,5,6,8-16].

In this study, we sought to clarify the immunologic (or other) basis of LAV-mediated protection against highly pathogenic SIV by statistical correlation of fundamental measures of LAV-elicited immunity with post-challenge efficacy in a large cohort of LAV-vaccinated rhesus macaques. Our approach was to vaccinate groups of macaques with different LAVs that vary in their level of attenuation and degree of amino acid sequence homology with the wildtype SIVmac239 challenge virus with the intent, at the level of the overall cohort, of producing sufficient heterogeneity in both immune responsiveness and protective efficacy to create a statistically powerful immune parameter vs. efficacy matrix. We focused on the most stringent route of SIV challenge – high dose intravenous administration – because 1) LAVs are unique among SIV vaccines in their ability to completely control such systemic SIV challenge[1-3], and 2) hematogenous dissemination is a common step in all primary HIV/SIV infections, including those arising from mucosal surfaces[17]. In this regard, a vaccine that intercepts and completely controls hematogenous HIV spread would be applicable to both mucosal and intravenous routes of HIV entry, the latter a clinically relevant way of acquiring infection that is not addressed by vaccines designed to elicit mucosal immunity. Strikingly, this experimental approach strongly and specifically identified characteristics of the SIV-specific T cell response in lymph node (including its magnitude, effector differentiation, functional properties and kinetics of activation after challenge) as cross-platform predictors of LAV-mediated protection against high dose

intravenous SIV challenge. We further linked the maintenance of these protective lymph node-based T cells to the ability of the replication-competent LAV to persist in follicular helper CD4+ T cells in secondary lymphoid tissues. Together, these findings provide further support for the concept that early SIV infection, even the systemically distributed infection following high dose intravenous challenge, is vulnerable to the high frequency, effector differentiated memory T cell responses that are uniquely elicited and maintained over the long term by persistent vectors.

RESULTS

Heterogeneous protection in rhesus macaques vaccinated with LAVs that vary in level of attenuation and/or sequence homology with the wildtype SIVmac239 challenge virus

To achieve the heterogeneity in both immune responses and protective efficacy necessary for robust statistical delineation of immune correlates, we selected LAV designs for study that vary in their level of attenuation and degree of amino acid sequence homology with the wildtype SIVmac239 challenge virus, and therefore would be expected to differ in the level and persistence of SIV antigens available to elicit adaptive immunity (leading to differences in magnitude, differentiation and durability of the T cell and antibody responses resulting from each vaccine), as well as in the ability of the resulting vaccine-elicited adaptive immunity to cross-react with the challenge virus. The prototype LAV, SIVmac239(Δnef), is only moderately attenuated, and is sequence-matched to the challenge virus. SIVmac239(Δ3) and single cycle SIVmac239 are also sequence-matched with the challenge virus, but are progressively more attenuated than SIVmac239(Δnef)[18,19]. SHIV89.6 is also only moderately attenuated, but differs from the SIVmac239(Δnef) prototype by virtue of highly heterologous, HIV-derived *env, tat, vpu* and *rev* sequences, and its ability to use CXCR4 as a co-receptor[5]. SIVsmE543(Δnef) is variably attenuated (due to its sensitivity to restrictive TRIM5 alleles), and is heterologous in amino acid sequence to SIVmac239 (~15% overall divergence)[13,20]. Each LAV was administered to 6-8 macaques to create an overall study group of 32 vaccinated animals (Fig. 1a). Macaques with class I major histocompatibility complex alleles associated with enhanced CD8+ T cell-mediated SIV control (*Mamu*-A*01, *Mamu*-B*08, and *Mamu*-B*17)[13] were excluded from this study to focus analysis on novel correlates of protection.

Consistent with the expected characteristics of the selected LAVs, the SHIV89.6-vaccinated macaques in our study group demonstrated the highest peak viremia, highest peak number of LAV RNA copies within peripheral blood mononuclear cells (PMBC), and most acute-phase effector-site CD4+ T cell depletion, followed by the macaques vaccinated with SIVmac239(Δnef), SIVmac239(Δ3), SIVsmE543(Δnef) and single-cycle SIVmac239 (Fig. 1b,c and Supplementary Fig. 1). Differences in these parameters were less apparent in chronic-phase , as the replication of even the least attenuated LAVs was brought under stringent control by week 10 after vaccination, and the modest acute-phase effector-site CD4+ T cell depletion was transient. Notably, however, the peak numbers of PBMC-associated LAV DNA copies established during acute-phase viremia decayed very slowly over time, providing a persistent measure of the amount of peak LAV replication (Fig. 1c).

After a 50-week vaccination period to allow full maturation and stabilization of anti-SIV immunity[2], the 32 LAV-inoculated, and six unvaccinated, control macaques were intravenously challenged with 10^3 infectious units of wildtype SIVmac239 (Fig. 1a). The LAV-vaccinated macaques in this study manifested three distinct outcomes after this challenge: 1) complete protection (n = 19), characterized by no significant net increase in overall plasma viral load (pvl), and either no detection of wildtype SIVmac239 with discriminatory qRT-PCR (n = 16) or transient, low level (< 10^3 copies ml^{-1}) detection (n = 3); 2) partial protection (n = 7), defined as clear establishment of wildtype SIV infection (> 10^4 copies ml^{-1} wildtype SIVmac239 RNA by discriminatory qRT-PCR and persistently elevated overall pvl), but with overall pvl reduced by at least 2 logs in the first 70 days post-challenge compared to unvaccinated controls; and 3) no protection (n = 6), in which post-challenge viral dynamics are indistinguishable from the unvaccinated controls (Fig. 1d). The biologic validity of these different outcome groups was confirmed by the observations that completely protected macaques lacked both an anamnestic T cell response to wildtype SIV challenge (a sensitive measure of increased SIV replication) and any evidence of SIV pathogenesis (e.g., loss of mucosal CD4$^+$ memory T cells), whereas partially protected and non-protected macaques manifested both unequivocal anamnestic responses and mucosal CD4$^+$ memory T cell depletion that was commensurate with their respective pvl levels (Fig. 1e,f). As expected, protection was highest in macaques vaccinated with LAVs that were the least attenuated and most homologous to the challenge virus (Fig. 1d). The peak plasma LAV load (initial 4 weeks after vaccination) and the chronic-phase plasma LAV load immediately before challenge, as well as the number of LAV DNA copies in PBMC immediately before challenge (which, as indicated above, closely correlates with peak LAV load in plasma) – all reflections of LAV attenuation – statistically delineated macaques at each end of the protection spectrum (in particular, completely vs. non-protected macaques; Fig. 1g,h). Notably, however, levels of PBMC-associated LAV RNA at the time of challenge did not significantly correlate with outcome (Fig. 1h).

SIV-specific T cell responses in lymph node predict challenge outcome

Prior to challenge, we quantified 11 primary parameters of SIV-specific immunity for assessment as potential correlates of protection, including three humoral immune parameters – SIVmac239 neutralization titres, native SIVenv binding titres (neutralization of tissue culture-adapted SIVmac251), and SIVenv-directed antibody-dependent cell-mediated cytotoxicity (all in plasma samples) – and eight T cell response parameters -- the magnitude of SIV proteome-specific CD4$^+$ and CD8$^+$ T cells in PBMC, bronchoalveolar lavage (BAL) fluid, and lymph node, as well as the breadth of these responses in PBMC. LAV-vaccinated macaques manifested a spectrum of values for each of these parameters, with the exception of SIVmac239 neutralizing antibody titres, which were detectable at low level in only a very small proportion of LAV-vaccinated animals (Suppl. Fig. 2). It is also noteworthy that SHIV89.6-vaccinated macaques lacked antibody responses to the heterologous SIVenv.

We next assessed each of these parameters for correlation with the outcome groups described above using the nonparametric Kruskal-Wallis test, adjusting for multiple comparisons using the Bonferroni method. Strikingly, only two parameters – the magnitude of SIV proteome-specific CD4$^+$ and CD8$^+$ responses in lymph node – statistically delineated

the outcome groups using this method (Table 1; Fig. 2a). Moreover, the SIV proteome-specific CD4^{+} and CD8^{+} T cell responses in lymph node were the only parameters to statistically delineate each of the three outcome groups from each other by the Wilcoxon rank sum test (Fig. 2a; Suppl. Fig. 3). In partially and non-protected macaques, the lymph node, but not the blood, SIV-specific T cell response magnitude (CD4^{+} and CD8^{+}) inversely correlated with peak viremia after challenge by Spearman analysis (Fig. 2b), indicating that pre-challenge, lymph node-based T cell responses also predict the degree of SIVmac239 control once infection with the wildtype virus is established. The majority of SIV-specific CD8^{+} T cells in pre-challenge lymph nodes of subsequently completely protected macaques manifested phenotypic evidence of both recent activation (HLA-DR and PD-1 expression) and effector differentiation (CCR5 expression) (Fig. 2c), suggesting an ability to manifest an immediate anti-viral effector response. To ascertain whether these SIV-specific T cells could directly mediate anti-SIV effector activity, we assessed the ability of sorted populations of memory T cells from PBMC and lymph node to suppress SIVmac239 replication *in vitro*. Indeed, CD8^{+} (but not CD4^{+}) memory T cells from lymph node (but not blood) of completely protected macaques manifested potent SIV suppression, and across the overall cohort, the level of this suppression strongly predicted each of the three outcome groups and inversely correlated with the peak post-challenge pvls in those macaques with establishment of wildtype SIVmac239 infection (Fig. 2d).

SIV-specific T cell responses in lymph node correlate with persistent LAV replication in follicular helper CD4^{+} T cells

The ability of efficacious LAVs to maintain protective T cell responses in lymph node appeared to depend on the preferential persistence of LAV replication in this tissue (Fig. 3a), as the magnitude of both the lymph node CD4^{+} and CD8^{+} SIV-specific T cell responses closely correlated with the level of cell-associated LAV RNA in lymph node (a measure of ongoing LAV replication; Fig. 3b). As these lymph node T cell responses correlated with protective efficacy (Fig. 2a-d), it is not surprising that the levels of cell-associated LAV RNA in lymph node prior to challenge also correlated with outcome after challenge (Fig. 3c). The preferential persistence of LAV in lymph node is explained by the highly selective replication of LAV in the CD4^{+}, PD-1^{hi}ICOS^{hi}CD200^{hi}CCR7^{low} follicular helper T cell (T$_{FH}$) subset (Fig. 3d; Suppl. Fig. 4), which are specifically localized in B cell follicles and therefore found almost exclusively in lymph node and other secondary lymphoid tissues[21-23].

Analysis of diverse tissues obtained at necropsy of 10 completely protected LAV-vaccinated macaques confirmed that B cell follicle-rich secondary lymphoid tissues, including lymph nodes, spleen and colonic mucosa, contained significantly higher copy numbers of cell-associated LAV RNA and DNA per 10^5 cells than primary lymphoid tissues (bone marrow) and extra-lymphoid tissues (jejunal mucosa, liver, BAL) that typically lack such B cell follicles (Fig. 3e). Strikingly, the mean frequencies of SIV-specific CD8^{+} T cells in each tissue closely correlated with the log mean of cell-associated SIV RNA in that tissue (Fig. 3f), an observation providing further evidence that the extent of ongoing LAV replication determines the frequency at which SIV-specific CD8^{+} T cells are maintained in any given tissue. Thus, CD4^{+} T$_{FH}$ cells serve as a sanctuary site for LAV persistence[23,24], and

concentrate LAV replication (and antigen production) in secondary lymphoid tissues, providing an immune stimulus for production and maintenance of SIV-specific T cells that is proportional to the level of T_{FH} infection.

Complete LAV-mediated protection is associated with increased memory T cell activation in lymph node at day 4 after challenge

Collectively, these data suggest that following intravenous challenge, lymph node and other secondary lymphoid tissues are major sites at which LAV-generated, SIV-specific T cells intercept the nascent wildtype SIV infection, and if these T cells are present in sufficient numbers, the wildtype SIV infection can be completely controlled and possibly cleared. To probe the dynamics and characteristics of the immune response at this putative intercept, we used microarray analysis to compare the transcriptional profiles of unfractionated lymph node cells obtained from completely protected, non-protected, and unvaccinated control macaques 7 days prior to, and 4 and 14 days after wildtype SIVmac239 challenge. Prior to challenge, the gene expression profiles of unfractionated lymph node cells from completely protected and non-protected macaques were indistinguishable from each other, but different from unvaccinated control macaques (Fig. 4a,b). Gene pathways that were significant in distinguishing vaccinated from non-vaccinated macaques included metabolic pathways associated with stress responses and survival (EIF2, mTOR, oxidative phosphorylation, protein ubiquitination), as well as pathways (NFAT, PLCγ, PKA and CD28) consistent with a low-level immune response to the LAV (Fig. 4c; Suppl. Table 1). Remarkably, at post-challenge day (PCD) 4 (a time point when cell-associated SIV RNA and DNA were not yet detectable in lymph nodes of the unvaccinated controls), the gene expression profiles of lymph node cells from completely protected and non-protected (but not control) macaques were dramatically different from pre-challenge, involving multiple pathways related to immune activation, but were still indistinguishable from each other (Fig. 4d-f; Suppl. Table 2). A gene-level comparison of PCD 4 vs. pre-challenge lymph node cells from completely protected, non-protected, and control macaques using an immune response gene filter revealed up-regulated T cell, inflammasome and antigen presenting cell gene activation, as well as genes regulating the innate/adaptive immunity interface in the vaccinated macaques compared to controls (Fig. 4g; Suppl. Discussion 1). Since the representation of the major cell subsets in lymph nodes of completely protected and non-protected macaques at PCD 4 was unchanged from baseline (Suppl. Fig. 5), these differences in gene expression profiles between baseline and PCD 4 probably reflect an *in situ* immune response. Moreover, given that the lymph node transcriptional profiles changed in vaccinated, but not unvaccinated control, macaques, they were almost certainly initiated by an adaptive (LAV-elicited) memory response to challenge. From PCD 4 to 14, the relationship between the transcriptional profiles of lymph nodes from completely protected, non-protected and control macaques changed (Fig. 4g; Suppl. Fig. 6). Consistent with the onset of progression of wildtype SIVmac239 infection in non-protected and control, but not completely protected, macaques, lymph node cells from the non-protected and control macaques showed similar patterns of gene expression associated with enhanced innate IFN and effector T and NK cell responses, whereas expression of immune related genes in lymph node cells from completely protected macaques was largely unaltered over this period (Suppl. Discussion 1).

To specifically compare the activity of memory T cells in the lymph nodes of completely vs. non-protected macaques following wildtype SIVmac239 challenge, we examined the transcriptional profiles of sorted CD8^{+} and CD4^{+} memory T cells from lymph nodes obtained at PCD 4 and 14. This analysis revealed that CD8^{+} memory T cells from PCD 4 lymph nodes of completely protected macaques manifested a relative up-regulation of TCR signaling genes and granzymes, and down-regulation of IL7R compared to non-protected macaques (Fig. 5), reflecting higher T cell activation and early establishment of CD8^{+} T cell effector responses in lymph nodes from these completely protected animals[25-27] (Suppl. Discussion 2). Although fewer gene expression changes distinguished CD4^{+} memory T cells from the lymph nodes of completely protected compared to nonprotected macaques at PCD 4, there was still significantly higher expression of genes associated with antigen-specific activation of CD4^{+} memory T cells in completely protected macaques, including CD40LG, LAG3, CTLA4, BTLA, and regulators of T cell survival (NFKB transcriptional pathway)[28,29] (Suppl. Fig. 7; Suppl. Discussion 2). By PCD 14, CD8^{+} memory T cells from non-protected macaques manifested transcriptional evidence of effector function[27], e.g., granzymes, as well as innate immune activation downstream of type 1 IFN signaling, protein ubiquitination and cellular proliferation pathways[30] (Fig. 5; Suppl. Tables 3,4), consistent with the late development of both adaptive and innate immune responses. CD4^{+} memory T cells from lymph node of non-protected macaques showed similarly increased expression of type I IFN response genes at PCD 14 (Suppl. Fig. 7). In contrast, CD8^{+} and CD4^{+} memory T cells from lymph nodes of completely protected macaques at PCD 14 manifested relative up-regulation of genes associated with long-term memory and cellular quiescence/survival[30,31] (Fig. 5; Supp. Fig. 7; Suppl. Table 3; Suppl. Discussion 2). Thus, transcriptional analysis of lymph node memory T cells provides evidence of larger and/or earlier CD8^{+} and CD4^{+} T cell response to challenge in completely protected vs. non-protected macaques (in keeping with the higher magnitude SIV-specific T cell responses in the lymph nodes of completely protected animals). This early response is associated with control of infection and prevention of the marked innate and adaptive immune activation that characterized progressive wildtype SIV infection.

DISCUSSION

Correlation analysis does not delineate cause and effect and, therefore, cannot unequivocally establish whether persistent LAV replication, the associated SIV-specific immune response or an uncharacterized covariate are mechanistically related to the observed protection. However, these data, taken together, lead most logically to a model in which persistent LAV replication elicits and maintains differentiated/activated, anti-viral effector memory T cells in tissues, and if these T cells are present in sufficient frequency prior to challenge, they can completely control (and perhaps clear) wildtype SIV infection in the first days after challenge. Secondary lymphoid tissues appear to be the critical site of viral intercept after intravenous challenge, and CD8^{+} memory T cells from lymph nodes of optimally LAV-vaccinated animals can strongly suppress wildtype SIV replication in autologous CD4^{+} T cells. Although CD4^{+} memory T cells from the lymph nodes of the same macaques lacked this capability, the very strong correlation between the frequency of SIV-specific CD4^{+} T cells in lymph node tissue and outcome suggests their crucial involvement in protection,

perhaps through direct effector activity against SIV-infected macrophages, help of SIV-specific, CD8^{+} T cell functionality or both[32,33]. Importantly, lymph node-based, SIV-specific T cell responses also delineated partial controllers from non-controllers, suggesting that when the LAV-elicited SIV-specific T cell responses are below the threshold for complete control, an anamnestic expansion of the LAV-elicited, SIV-specific memory T cells can ensue, with the outcome determined, as with conventional prime-boost vaccines, by a competition between the kinetics and anti-viral activity of the anamnestic response and viral escape[4].

Viral interference probably does not substantially contribute to observed protection given that LAV replication is restricted largely to CD4^{+} T_{FH} cells, a minor subset of the total potential population of CD4^{+} target cells. Innate immunity elicited by persistent LAV replication is another candidate mechanism for mediating protection. Although our sampling schedule may have missed a transient innate immune response, our detailed transcriptional analysis revealed no evidence of differential innate immune activation in the lymph nodes of protected compared to unprotected macaques before challenge or at 4 days after challenge and thereby argues against this possibility. In addition, the number and activation status of NK cells in lymph node prior to, or following, challenge did not correlate with protection, arguing against involvement of these innate immune effectors (Suppl. Fig. 8). Perhaps the most compelling evidence in support of the T cell protection model of LAV efficacy is the analogous immediate and complete, MHC I allele-independent control of SIV infection that is associated with the high frequency, tissue-based, SIV-specific T cell responses elicited and maintained by SIV protein-expressing cytomegalovirus vectors[34]. These persistent β-herpesvirus vectors have a completely different biology than LAV (target cell tropism, innate immune interaction, immune evasion and persistence strategies) and do not elicit antibody responses to SIV inserts, factors strongly implicating tissue-based, effector-differentiated memory T cells as the common mediator of protection with these persistent vectors.

In summary, these data identify the magnitude of SIV-specific CD4^{+} and CD8^{+} T cell responses in secondary lymphoid tissues (but notably, not blood), as well as the SIV suppression capacity of CD8^{+} memory T cells in these tissues, as strong (cross-platform) correlates of LAV-mediated protection. These results do not preclude other innate or adaptive immune mechanisms (including antibodies) as potential contributors to LAV efficacy, especially at mucosal surfaces[16], or to protection from mucosal challenge afforded by other vaccine modalities, as has been suggested recently in both clinical[35] and NHP studies[36]. However, taken together, these observations provide further support for the conclusion that effector-differentiated, SIV-specific memory T cells, when maintained at a high frequency in tissues important for SIV infection, can intercept and completely control a nascent, highly pathogenic SIV infection without anamnestic expansion[15,34]. This intercept and control may occur at mucosal sites of entry, lymphoid tissues that are involved in early spread (the latter even when mucosal infection is bypassed by intravenous inoculation) or both, but they always occur before the establishment of a 'critical mass' of replication virus that is capable of dynamic evolution and immune escape[4]. To date, this pattern of protection has been consistently observed only with LAVs or SIV vaccines that are based on persistent cytomegalovirus vectors. These findings therefore support the exploitation of tissue-based,

effector-differentiated memory T cell responses and their associated immediate and complete protection by the development of HIV and AIDS vaccines that are based on persistent, nonpathogenic vectors or on other strategies that are capable of eliciting and maintaining such effector memory T cell responses[37].

METHODS

Animals

A total of 38 adult male rhesus macaques (*Macaca mulatta*) of Indian genetic background were used in this study. All macaques were free of cercopethicine herpesvirus 1, simian type D retrovirus, simian T-lymphotropic virus type 1 and SIV infection at the start of the study, and were used with approval of the Oregon National Primate Research Center's Animal Care and Use Committee, under the standards of the NIH Guide for the Care and Use of Laboratory Animals. Macaques with major histocompatibility complex alleles (*Mamu*-A*01, *Mamu*-B*08 and *Mamu*-B*17), which have previously been associated with spontaneous and/or LAV-associated control of wildtype SIV[13], were excluded from this study.

Viruses

SIVmac239(Δnef)[1], SIVmac239(Δ3)[18], SHIV89.6[5], and SIVsmE543(Δnef) were given to 6-8 macaques each intravenously at a dose of 3×10^4 focus forming units (ffu), 2×10^5 ffu, 2×10^3 ffu, and 3×10^4 ffu, respectively (all replicating SIV stocks quantified using the sMAGI cell assay[41]). SIVsmE543(Δnef) has a truncated Nef protein (the first N-terminal 58 amino acids flanked by C-terminal 16 amino acids VSFYKRKGGTGRDLLQ derived from SIVmac239). Single cycle SIVmac239[19] was given intravenously three times at a dose of 5μg p27 each (by ELISA) at weeks 0, 4, and 8. All macaques were intravenously challenged with PBMC-expanded SIVmac239 at a dose of 1000 ffu at 50 weeks after LAV vaccination, with the exception of two SIVsmE543(Δnef)-vaccinated macaques that were challenged at 73 weeks post-vaccination using the same stock of wild-type SIVmac239 challenge virus.

Cell processing

Mononuclear cell preparations were obtained from blood, bone marrow, BAL, lymph nodes, spleen, liver, jejunum and colon as previously described [38,42,43]. For cell-associated viral load determination, 1×10^6 cells were pelleted and frozen immediately in liquid nitrogen and then stored at −80°C until use. For the transcriptional analysis of lymph node, unfractionated lymph node mononuclear cells (1×10^6) or sorted lymph node cells (harvested at 7 days before and 4 and 14 days after challenge) were resuspended in RLT lysis buffer (Qiagen) and stored at −80°C until use. CD4^{+} and CD8^{+} memory T cells were isolated by sorting on a FACS Aria II (BD Biosciences) on the basis of cell surface staining patterns of the lineage markers CD3, CD4, CD8, and memory markers CD95 and CD28, using previously described criteria[38]. In some studies, CD4^{+} memory T cells were further sorted based on expression levels of PD-1 using mAb eBioJ105 (eBioscience).

Viral quantification

Quantitative PCR and RT-PCR assays targeting a highly conserved nucleic acid sequence in gag were used for standard measurement of plasma SIV RNA and cell-associated SIV RNA/DNA in PBMC and cells isolated from tissues, as previously described[44,45]. The primers and probes used to discriminate SIVmac239 from SIVmac239(Δnef) and SIVmac239(Δ3) were described previously[46]. Potential mixtures of SIVsmE543(Δnef) and SIVmac239 were assayed using the SIVsmE543 *gag*-specific primers 5′-GCAGGGCAACTTAGAGAGCCAAG-3′ and 5′-TGGTAT(G/A)GGGTTTTGTTGCCTG-3′ and probe 5′CalFluor®Red610-TAGTTCCTGCAATGTCTGAT C-BHQ®2 and the SIVmac239 gag-specific primers 5′-GAGGCCCTCGCACCAGTG-3′ and 5′-CATGGTCCATTTTTCCACATTTC-3′ and probe 5′Quasar® 670-CAATCCCTTTTGCAGCAGCCCAACAG-BHQ®2. Potential mixtures of SHIV89.6 and SIVmac239 were assayed using the SHIV*env* parental construct *vpu*-specific primers 5′-CTTTCATTGCCAAGTTTGTTTCATAAC-3′ and 5′-TCGTCGCTGTCTCCGCTTC-3′ and probe 5′Quasar®670-AAAGCCTTAGGCATCTCCTATGGCAGGA-BHQ®2 and the SIVmac239 *env*-specific primers 5′-GCApTTCAGAGGpGGATGC-3′ and 5′-CCCAAGACATCCCATACATTACTTGT-3′ and probe 5′CalFluor® Orange-ACTCCAGAATCGGCCAkpCTGGk-BHQ®1 where p and k bases (Glen Research) refer to pyrimidine and purine analogs, respectively, that permit pairing at base-divergent positions. All assays were optimized for maximal sensitivity of specific target detection of 5 copy equivalents per test reaction (95% assurance) and validated for minimum discriminate ratios of 10^5:1 for the indicated potential mixtures of virus sequences. The presence of inducible, replication competent LAV was detected in whole lymph node mononuclear cell preparations (or sorted cell populations obtained as described above) by co-cultivation of these cells with CEMx174 cells[40], using flow cytometric analysis of intra-cellular SIVgag p27 (using SIVmac251 p27-specific mAb, ABL, Inc.) to detect infection[47].

T cell assays

SIV-specific T cells were enumerated in mononuclear cells isolated from blood and tissues by flow cytometric intracellular cytokine analysis, as previously described in detail[48]. Briefly, mixes of sequential (11 amino acid overlapping) 15-mer peptides (AnaSpec) spanning the SIVmac239 gag, env, pol, nef, rev/tat, vif/vpr/vpx were used as antigens in conjunction with anti-CD28 (BD Biosciences) and CD49d co-stimulatory monoclonal antibodies (BD Biosciences). For the transcriptional analysis of lymph node, unfractionated lymph node mononuclear cells (1×10^6) or sorted lymph node cells (harvested at 7 days before and 4 and 14 days after challenge) were resuspended in RLT lysis buffer (Qiagen) and stored at −80 °C until use. Co-stimulation in the absence of peptides served as background control. Cells were stained with fluorochrome-conjugated monoclonal antibodies, and data were collected on an LSRII (BD Biosciences) and analyzed using the FlowJo software program (version 8.8.6; Tree Star, Inc.). Response frequencies ($CD69^+TNF$-α^+ and/or $CD69^+IFN$-γ^+) were first determined in the overall $CD4^+$ and $CD8^+$ population and then memory corrected (memory subset populations were delineated on the basis of CD28 and CD95 expression)[48]. The sum of net response frequencies determined for

each peptide mix described above was considered the overall (pan-proteome) SIV-specific response frequency. To measure breadth of SIV-specific T cell responses in PBMC, we determined the frequency of CD4^{+} and CD8^{+} T cells that were responsive to 82 separate pools of ten 15mer peptides consisting of SIVmac239 proteins (env, pol, gag, nef, rev, tat, vif, vpr, and vpx with 22, 26, 13, 6, 2, 3, 5, 2, and 3 pools, respectively).Breadth was reported as the number of 10-peptide mixes with an above-threshold (0.05%) response. To determine the cell surface phenotype of SIV-specific CD8^{+} T cells, mononuclear cells were stimulated as described above, except that the CD28 co-stimulatory mAb was used as a fluorochrome conjugate to allow CD28 expression levels to be assessed by flow cytometry. After incubation, cells were stained on the surface for lineage markers (CD3, CD4, CD8) and memory/activation markers (CCR5, PD-1, HLA-DR) prior to fixation/permeabilization and then intracellular staining for response markers (IFN-γ, TNF-α). Viral suppression assays were based on the approach of Martins, *et al.*[47]. Briefly, autologous CD4^{+} T cells were isolated from PBMC by NHP CD4^{+} T cell isolation kits (Miltenyi Biotec), activated *in vitro* with staphylococcal enterotoxin B (1 μg ml^{-1}; Sigma), anti-CD3, anti-CD28, and anti-CD49d antibodies, infected with SIVmac239 stock by centrifugation (1200g for 2 h, 30°C) and labeled with CFSE (2.5 μM) for 10 min at 37°C. These target cells were incubated with (or without) effector cells (sorted CD4^{+} or CD8^{+} memory T cells, obtained as described above) at an effector:target ratio of 1:1 memory for 72 h, and the percentage of SIVgag p27^{+} cells in the CFSE[+] subset was determined by flow cytometric analysis of intra-cellular SIVgag p27 staining (mAb 55-2F12, NIH AIDS Research and Reference Reagent Program). The %viral suppression was calculated by the formula; 100 - (%p27 with effectors - %p27 in uninfected target cells) / (%p27 without effectors - %p27 in uninfected target cells) × 100. T cell phenotype was performed by flow cytometry as previously described[49], using established criteria for memory T subsets, activated T cells and follicular helper T cells[21,22,39,46,50,51].

Antibody response assays

Neutralizing antibodies against SIVmac239 and tissue culture-adapted SIVmac251 were quantified in luciferase reporter gene assays using the TZM-bl and M7 Luc cell lines, respectively[52]. SIVenv-specific antibodies with antibody-dependent cell-mediated cytotoxicity activity were measured as described[53].

Microarray analysis

RNA was isolated using RNeasy Micro Kits (Qiagen) and the quantity and quality confirmed using a NanoDrop 2000c (Thermo Fisher Scientific) and an Experion Electrophoresis System. Samples (50 ng) were amplified using Illumina TotalPrep RNA amplification kits (Ambion). Microarray analysis was conducted using 750 ng of biotinylated cRNA hybridized to HumanHT-12_V4 BeadChips (Illumina) at 58°C for 20 h. The arrays were scanned using Illumina's iSCAN and quantified using Genome Studio (Illumina). Analysis of the GenomeStudio output data was conducted using R (R Development Core Team)[54] and Bioconductor[55] software packages. Quantile normalization was applied, followed by a log$_2$ transformation. The LIMMA package[56] was used to fit a linear model to each probe and to perform (moderated) t-tests or F-tests on the compared groups. To control the expected proportions of false positives, the FDR for each unadjusted

P value was calculated using the Benjamini and Hochberg method implemented in LIMMA. Multidimensional scaling was used as a dimensionality reduction method in R to generate plots for evaluation of similarities or dissimilarities between data sets. Ingenuity Pathway Analysis software (IPA, Ingenuity Systems) was used to annotate genes and rank canonical pathways. An immune response gene filter, constructed from innate and adaptive immune response gene queries of Gene Ontology (www.geneontology.org), T cell activation and complement pathway genes from IPA, and our own IFN- and inflammasome-response gene lists[57] was used where noted to reduce datasets for visualization prior to FDR estimation. The microarray data are available through the National Center for Biotechnology Information Gene Expression Omnibus (GEO superseries GSE40006).

Statistical analysis

The goal of the primary statistical analysis was to predict post-challenge outcome from pre-challenge immune response variables (responses to the LAVs). The primary measure of outcome was the ordinal protection variable, the categories of which – completely protected, partially protected and non-protected – were determined and validated as described in the Results section. The eleven primary independent potential immune response predictors are summarized in Table 1. In all cases, we used immunologic values obtained from samples collected at the closest available time point before the challenge. To determine which, if any, of these immune response parameters predict outcome, we used univariate, nonparametric Kruskal-Wallis tests to assess each of the 11 primary predictor (immunologic) variables vs. the three protection categories. We considered a parameter to be a correlate of predictor of outcome if the *P* value resulting from this analysis was less than 0.05 after Bonferroni-correction for multiple comparisons. In follow-up analyses, we conducted Wilcoxon rank sum tests to compare predictors across pairs of the three protection categories. In addition, to analyze the degree of protection in those macaques with establishment of the wildtype SIVmac239 virus after challenge (partially protected and non-protected groups), we used the Spearman test to conduct nonparametric correlation analysis of immune parameters with a quantitative measure of outcome, the "maximum ΔPlasma Viral Load" (max. Δ pvl), which is the log10-transformed difference between the maximum of the post-challenge peak pvl (from PCD 4, 7, 10, 14, 21, 28) and the average baseline pvl (mean of pre-challenge time points: day −14, −4, and 0). We conducted all follow-up and secondary or exploratory statistical analyses without multiplicity correction, using nonparametric tests: Kruskal-Wallis, Wilcoxon, and Spearman tests for categorical, dichotomous, and correlation tests, respectively[58]. When comparing cell-associated viral load across tissue types, we applied Wilcoxon signed rank tests to the within-animal differences across tissues. We used R for all statistical analyses[54].

Supplementary Material

Refer to Web version on PubMed Central for supplementary material.

ACKNOWLEDGMENTS

REFERENCES

1. Daniel MD, Kirchhoff F, Czajak SC, Sehgal PK, Desrosiers RC. Protective effects of a live attenuated SIV vaccine with a deletion in the nef gene. Science. 1992; 258:1938–1941. [PubMed: 1470917]

2. Johnson RP, Desrosiers RC. Protective immunity induced by live attenuated simian immunodeficiency virus. Curr Opin Immunol. 1998; 10:436–443. [PubMed: 9722920]

3. Koff WC, et al. HIV vaccine design: insights from live attenuated SIV vaccines. Nat Immunol. 2006; 7:19–23. [PubMed: 16357854]

4. Picker LJ, Hansen SG, Lifson JD. New Paradigms for HIV/AIDS Vaccine Development. Annu Rev Med. 2011; 63:95–111. [PubMed: 21942424]

5. Abel K, et al. Simian-human immunodeficiency virus SHIV89.6-induced protection against intravaginal challenge with pathogenic SIVmac239 is independent of the route of immunization and is associated with a combination of cytotoxic T-lymphocyte and alpha interferon responses. J Virol. 2003; 77:3099–3118. [PubMed: 12584336]

6. Sugimoto C, et al. Protection of macaques with diverse MHC genotypes against a heterologous SIV by vaccination with a deglycosylated live-attenuated SIV. PLoS One. 2010; 5:e11678. [PubMed: 20652030]

7. Whitney JB, Ruprecht RM. Live attenuated HIV vaccines: pitfalls and prospects. Curr Opin Infect Dis. 2004; 17:17–26. [PubMed: 15090885]

8. Metzner KJ, et al. Effects of in vivo CD8(+) T cell depletion on virus replication in rhesus macaques immunized with a live, attenuated simian immunodeficiency virus vaccine. J Exp Med. 2000; 191:1921–1931. [PubMed: 10839807]

9. Stebbings R, et al. Vaccination with live attenuated simian immunodeficiency virus for 21 days protects against superinfection. Virology. 2004; 330:249–260. [PubMed: 15527850]

10. Stebbings R, et al. CD8+ lymphocytes do not mediate protection against acute superinfection 20 days after vaccination with a live attenuated simian immunodeficiency virus. J Virol. 2005; 79:12264–12272. [PubMed: 16160152]

11. Nethe M, Berkhout B, van der Kuyl AC. Retroviral superinfection resistance. Retrovirology. 2005; 2:52. [PubMed: 16107223]

12. Schmitz JE, et al. Effect of CD8+ lymphocyte depletion on virus containment after simian immunodeficiency virus SIVmac251 challenge of live attenuated SIVmac239delta3-vaccinated rhesus macaques. J Virol. 2005; 79:8131–8141. [PubMed: 15956558]

13. Reynolds MR, et al. Macaques vaccinated with live-attenuated SIV control replication of heterologous virus. J Exp Med. 2008; 205:2537–2550. [PubMed: 18838548]

14. Mansfield K, et al. Vaccine protection by live, attenuated simian immunodeficiency virus in the absence of high-titer antibody responses and high-frequency cellular immune responses measurable in the periphery. J Virol. 2008; 82:4135–4148. [PubMed: 18272584]

15. Genesca M, et al. With minimal systemic T-cell expansion, CD8+ T Cells mediate protection of rhesus macaques immunized with attenuated simian-human immunodeficiency virus SHIV89.6 from vaginal challenge with simian immunodeficiency virus. J Virol. 2008; 82:11181–11196. [PubMed: 18787003]

16. Reynolds MR, et al. Macaques vaccinated with simian immunodeficiency virus SIVmac239Delta nef delay acquisition and control replication after repeated low-dose heterologous SIV challenge. J Virol. 2010; 84:9190–9199. [PubMed: 20592091]

17. Haase AT. Early events in sexual transmission of HIV and SIV and opportunities for interventions. Annu Rev Med. 2011; 62:127–139. [PubMed: 21054171]

18. Johnson RP, et al. Highly attenuated vaccine strains of simian immunodeficiency virus protect against vaginal challenge: inverse relationship of degree of protection with level of attenuation. J Virol. 1999; 73:4952–4961. [PubMed: 10233957]

19. Jia B, et al. Immunization with single-cycle SIV significantly reduces viral loads after an intravenous challenge with SIV(mac)239. PLoS Pathog. 2009; 5:e1000272. [PubMed: 19165322]

20. Kirmaier A, et al. TRIM5 suppresses cross-species transmission of a primate immunodeficiency virus and selects for emergence of resistant variants in the new species. PLoS Biology. 2010; 8:e1000462. [PubMed: 20808775]

21. Crotty S. Follicular helper CD4 T cells (TFH). Annu Rev Immunol. 2011; 29:621–663. [PubMed: 21314428]

22. Ma CS, et al. Early commitment of naive human CD4(+) T cells to the T follicular helper (T(FH)) cell lineage is induced by IL-12. Immunol Cell Biol. 2009; 87:590–600. [PubMed: 19721453]

23. Hong JJ, Amancha PK, Rogers K, Ansari AA, Villinger F. Spatial alterations between CD4^{+} T follicular helper, B, and CD8^{+} T cells during simian immunodeficiency virus infection: T/B cell homeostasis, activation, and potential mechanism for viral escape. J Immunol. 2012; 188:3247–3256. [PubMed: 22387550]

24. Sugimoto C, et al. nef gene is required for robust productive infection by simian immunodeficiency virus of T-cell-rich paracortex in lymph nodes. J Virol. 2003; 77:4169–4180. [PubMed: 12634375]

25. West EE, et al. Tight regulation of memory CD8(+) T cells limits their effectiveness during sustained high viral load. Immunity. 2011; 35:285–298. [PubMed: 21856186]

26. Kallies A. Distinct regulation of effector and memory T-cell differentiation. Immunol Cell Biol. 2008; 86:325–332. [PubMed: 18362944]

27. Intlekofer AM, et al. Effector and memory CD8^{+} T cell fate coupled by T-bet and eomesodermin. Nat Immunol. 2005; 6:1236–1244. [PubMed: 16273099]

28. Taylor JJ, Jenkins MK. CD4^{+} memory T cell survival. Curr Opin Immunol. 2011; 23:319–323. [PubMed: 21524898]

29. Kersse K, Lamkanfi M, Bertrand MJ, Vanden Berghe T, Vandenabeele P. Interaction patches of procaspase-1 caspase recruitment domains (CARDs) are differently involved in procaspase-1 activation and receptor-interacting protein 2 (RIP2)-dependent nuclear factor kappaB signaling. J Biol Chem. 2011; 286:35874–35882. [PubMed: 21862576]

30. Verdeil, G.g.; Puthier, D.; Nguyen, C.; Schmitt-Verhulst, A-M.; Auphan-Anezin, N. STAT5-Mediated Signals Sustain a TCR-Initiated Gene Expression Program toward Differentiation of CD8 T Cell Effectors. J Immunol. 2006; 176:4834–4842. [PubMed: 16585578]

31. Coller HA, Sang L, Roberts JM. A New Description of Cellular Quiescence. PLoS Biol. 2006; 4:e83. [PubMed: 16509772]

32. Sacha JB, et al. Gag- and Nef-specific CD4^{+} T cells recognize and inhibit SIV replication in infected macrophages early after infection. Proc Natl Acad Sci U S A. 2009; 106:9791–9796. [PubMed: 19478057]

33. Sant AJ, McMichael A. Revealing the role of CD4^{+} T cells in viral immunity. J Exp Med. 2012; 209:1391–1395. [PubMed: 22851641]

34. Hansen SG, et al. Profound early control of highly pathogenic SIV by an effector memory T-cell vaccine. Nature. 2011; 473:523–527. [PubMed: 21562493]

35. Haynes BF, et al. Immune-correlates analysis of an HIV-1 vaccine efficacy trial. N Engl J Med. 2012; 366:1275–1286. [PubMed: 22475592]

36. Barouch DH, et al. Vaccine protection against acquisition of neutralization-resistant SIV challenges in rhesus monkeys. Nature. 2012; 482:89–93. [PubMed: 22217938]

37. Vezys V, et al. Memory CD8 T-cell compartment grows in size with immunological experience. Nature. 2009; 457:196–199. [PubMed: 19005468]

38. Pitcher CJ, et al. Development and homeostasis of T cell memory in rhesus macaque. J Immunol. 2002; 168:29–43. [PubMed: 11751943]

39. Grossman Z, Picker LJ. Pathogenic mechanisms in simian immunodeficiency virus infection. Curr Opin HIV AIDS. 2008; 3:380–386. [PubMed: 19372994]

40. Shen A, et al. Novel pathway for induction of latent virus from resting CD4(+) T cells in the simian immunodeficiency virus/macaque model of human immunodeficiency virus type 1 latency. J Virol. 2007; 81:1660–1670. [PubMed: 17151130]

41. Chackerian B, Haigwood NL, Overbaugh J. Characterization of a CD4-expressing macaque cell line that can detect virus after a single replication cycle and can be infected by diverse simian immunodeficiency virus isolates. Virology. 1995; 213:386–394. [PubMed: 7491763]

42. Veazey RS, et al. Gastrointestinal tract as a major site of CD4$^+$ T cell depletion and viral replication in SIV infection. Science. 1998; 280:427–431. [PubMed: 9545219]

43. Schmitz JE, et al. Simian immunodeficiency virus (SIV)-specific CTL are present in large numbers in livers of SIV-infected rhesus monkeys. J Immunol. 2000; 164:6015–6019. [PubMed: 10820285]

44. Cline AN, Bess JW, Piatak M Jr. Lifson JD. Highly sensitive SIV plasma viral load assay: practical considerations, realistic performance expectations, and application to reverse engineering of vaccines for AIDS. J Med Primatol. 2005; 34:303–312. [PubMed: 16128925]

45. Venneti S, et al. Longitudinal in vivo positron emission tomography imaging of infected and activated brain macrophages in a macaque model of human immunodeficiency virus encephalitis correlates with central and peripheral markers of encephalitis and areas of synaptic degeneration. Am J Pathol. 2008; 172:1603–1616. [PubMed: 18467697]

46. Salisch NC, et al. Inhibitory TCR coreceptor PD-1 is a sensitive indicator of low-level replication of SIV and HIV-1. J Immunol. 2010; 184:476–487. [PubMed: 19949078]

47. Martins MA, et al. T-cell correlates of vaccine efficacy after a heterologous simian immunodeficiency virus challenge. J Virol. 2010; 84:4352–4365. [PubMed: 20164222]

48. Hansen SG, et al. Effector memory T cell responses are associated with protection of rhesus monkeys from mucosal simian immunodeficiency virus challenge. Nat Med. 2009; 15:293–299. [PubMed: 19219024]

49. Walker JM, Maecker HT, Maino VC, Picker LJ. Multicolor flow cytometric analysis in SIV-infected rhesus macaque. Methods Cell Biol. 2004; 75:535–557. [PubMed: 15603441]

50. Picker LJ, et al. IL-15 induces CD4 effector memory T cell production and tissue emigration in nonhuman primates. J Clin Invest. 2006; 116:1514–1524. [PubMed: 16691294]

51. Picker LJ, et al. Control of lymphocyte recirculation in man. I. Differential regulation of the peripheral lymph node homing receptor L-selectin on T cells during the virgin to memory cell transition. J Immunol. 1993; 150:1105–1121. [PubMed: 7678616]

52. Todd CA, et al. Development and implementation of an international proficiency testing program for a neutralizing antibody assay for HIV-1 in TZM-bl cells. J Immunol Methods. 2011

53. Pollara J, et al. High-throughput quantitative analysis of HIV-1 and SIV-specific ADCC-mediating antibody responses. Cytometry A. 2011; 79:603–612. [PubMed: 21735545]

54. R Development Core Team. R, A Language and Environment for Statistical Computing. 2011. http://www.R-project.org

55. Gentleman RC, et al. Bioconductor: open software development for computational biology and bioinformatics. Genome Biol. 2004; 5:R80. [PubMed: 15461798]

56. Smyth GK. Linear models and empirical bayes methods for assessing differential expression in microarray experiments. Stat Appl Genet Mol Biol. 2004; 3 Article#3.

57. Caskey M, et al. Synthetic double-stranded RNA induces innate immune responses similar to a live viral vaccine in humans. J Exp Med. 2011; 208:2357–2366. [PubMed: 22065672]

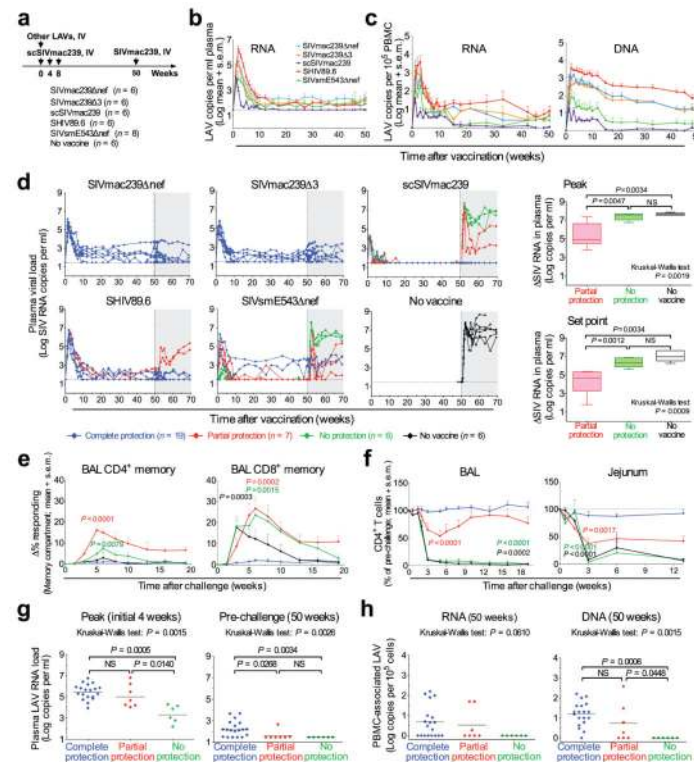58. Wolfe, DA.; Hollander, M. Nonparametric Statistical Methods. Wiley; New York: 1973.

Figure 1. LAV virology and differential efficacy

(**a**) Schematic illustrating the vaccination and challenge protocol and rhesus macaque groups (IV = intravenous). (**b**) Comparison of plasma LAV RNA levels and (**c**) the PBMC-associated LAV RNA and DNA levels of the different LAV-vaccinated macaque groups during the vaccine phase. (**d**) Effect of wildtype SIVmac239 challenge on overall plasma SIV RNA levels of LAV-vaccinated vs. unvaccinated control macaques (shaded area = after challenge). Each LAV-vaccinated macaque was categorized into a protection group: complete, partial or no protection (see main text). At right, two whisker plots (median, 25th/75th percentile, minimum/maximal value) compare the Δ peak and Δ set point pvls – the log10-transformed difference between the pre-challenge pvl and either the peak pvl in first 4 weeks, or the set point pvl at 13-19 weeks post challenge – in the partially protected, non-protected, and unvaccinated groups (note: completely protected macaques had no net Δ pvl after challenge), with the significance of overall differences in these values determined by the Kruskal-Wallis test and pair-wise differences with the Wilcoxon rank sum test when the Kruskal-Wallis *P* value was < 0.05 (NS = non-significant). (**e**) Analysis of the change in the overall SIV-specific CD4+ and CD8+ T cell responses in BAL fluid of the designated protection groups after challenge (mean + s.e.m). We compared the maximal change in these response frequencies after challenge (response peak) in the partially protected, non-protected and unvaccinated macaques to that of the completely protected macaques at the same time point by the Wilcoxon rank sum test with significant *P* values (< 0.05) shown. (**f**) Analysis of the post-challenge depletion of CD4+ memory T cells (mean + s.e.m) in the designated protection groups in BAL and jejunal mucosa (pre-challenge baseline normalized to 100%; statistical analysis as in e). (**g**) Comparison of the peak and pre-challenge plasma LAV loads in the 3 protection groups (statistical analysis as described in d). (**h**) Comparison of pre-

challenge PBMC-associated LAV RNA and DNA levels in the 3 protection groups (statistical analysis as described in d).
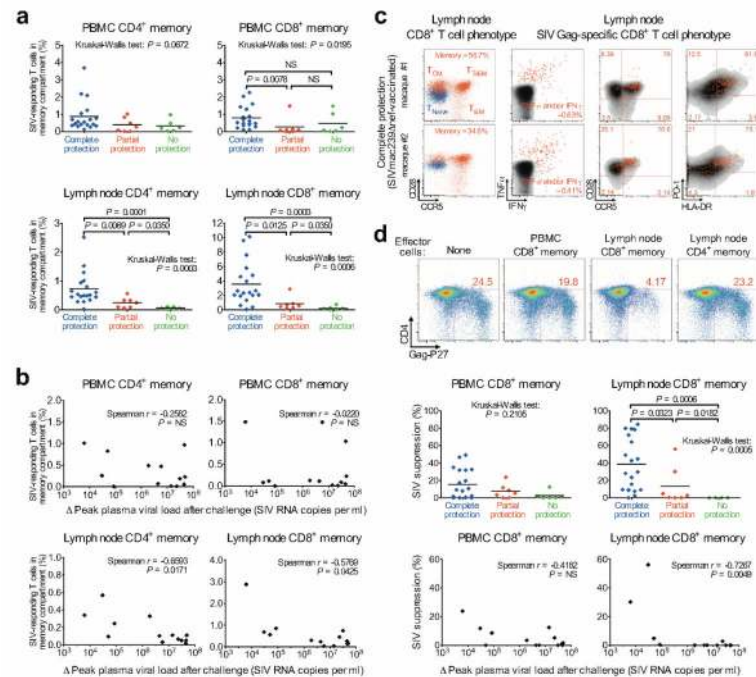
Figure 2. Immunological correlates of LAV-mediated protection

(**a**) Comparison of the pre-challenge magnitude of the total SIV-specific CD4^{+} and CD8^{+} T cell responses in the PBMC or lymph node memory compartment of the designated protection groups with the significance of overall differences in these values determined by the Kruskal-Wallis test and pair-wise differences with the Wilcoxon rank sum test when the Kruskal-Wallis *P* value was <0.05 (horizontal bars show mean values; NS = non-significant). (**b**) Spearman analysis of the correlation between the pre-challenge magnitude of the total SIV-specific CD4^{+} and CD8^{+} T cell responses in the PBMC or lymph node memory compartment and peak Δ pvl post-challenge among the partially and non-protected macaques (*n* = 13 total). (**c**) Flow cytometric analysis of phenotype of overall (*left*) and SIVgag-specific (*right*) CD8^{+} T cells from pre-challenge lymph nodes of two representative LAV-vaccinated, completely protected macaques. The profiles shown were gated on CD3^{+}CD8^{+} small lymphocytes. In the left panel, the naïve (*blue*) and total memory (*red*) subsets were determined by criteria based on CD28 vs. CD95 expression and the memory subsets – central memory, T_{CM}; transitional effector memory, T_{TrEM}; and effector memory, T_{EM} – determined by CD28 vs. CCR5 expression[38,39]. In the right panels, gag-responsive cells (*red*) were identified by intra-cellular expression of TNF-α and/or IFN-γ (total %+ shown) and then characterized for their cell-surface expression of CD28 vs. CCR5, PD-1 vs. HLA-DR (quadrant markers based on negative control staining with the % of events in each quadrant shown). (**d**) Analysis of the ability of isolated memory T cells from LAV-vaccinated macaques to suppress SIVmac239 replication in autologous CD4^{+} T cells. The top panels show results from a representative completely protected macaque. The middle panels compare pre-challenge levels of viral suppression by sorted CD8^{+} memory T cells from PBMC vs. lymph node for the designated protection groups with the significance of differences between groups analyzed as described in a. The bottom panels show Spearman analysis of the correlation between the level of viral suppression by sorted CD8^{+} memory T

cells from PBMC or lymph node and Δ peak pvl post-challenge among partially protected and non-protected macaques (n = 13 total).
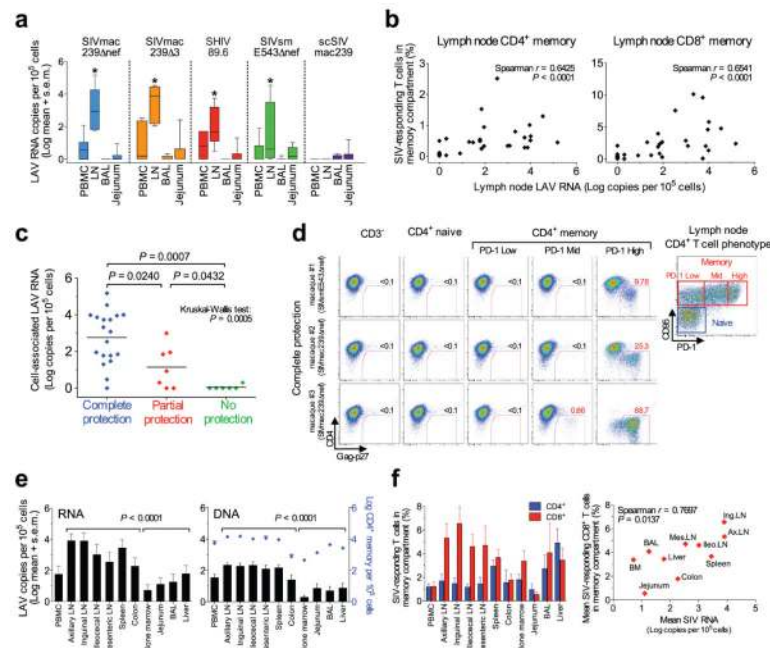
Figure 3. Association of tissue LAV replication and SIV-specific T cell responses
(**a**) The whisker plot (median, 25th/75th percentile, minimum/maximal value) compares the pre-challenge levels of cell-associated LAV RNA in mononuclear cells from blood, lymph node, BAL and jejunal mucosa in macaques vaccinated with the designated LAV. Asterisks indicate significantly higher levels of LAV RNA in the lymph node compared to the other three tissues by the Wilcoxon Signed Rank test ($P \leq 0.05$). (**b**) Spearman analysis of the correlation between pre-challenge levels of cell-associated LAV RNA in unfractionated lymph node cells and pre-challenge magnitude of the total SIV-specific T cell responses in the CD4+ and CD8+ lymph node memory compartments. (**c**) Comparison of the pre-challenge levels of cell-associated LAV RNA in lymph node cells in the designated protection groups with statistical analysis as described in Figure 2a (horizontal bars show mean values). (**d**) Isolation of replication-competent LAV from the designated sorted, pre-challenge lymph node cell populations (inset at right) from 3 representative, completely protected macaques using CEMx174 co-culture (22 days; 10^4 sorted lymph node cells and 10^5 CEMx174 target cells/culture) with detection of infection by flow cytometric analysis of intra-cellular SIVgag p27[40]. (**e**) Analysis of cell-associated SIV RNA and DNA ($\log_{10}$ mean + s.e.m.) in mononuclear cells obtained from the designated tissues of ten completely protected macaques at necropsy (all macaques negative for wildtype SIV RNA/DNA by discriminatory RT-PCR/PCR in lymph node cells; LN = lymph node). Blue diamond symbols in the right panel indicate the number of CD4+ memory T cells (potential SIV target cells) per 10^5 mononuclear cells in each tissue (*right y-axis*). The levels of cell-associated SIV RNA or DNA in secondary lymphoid tissues (B cell follicle-rich; all lymph nodes, spleen and colonic mucosa) were compared to that found in non-secondary lymphoid tissues (B cell follicle-poor; bone marrow, BAL, liver, jejunal mucosa) of these completely protected macaques by the Wilcoxon rank sum test with the *P* values shown. (**f**) The mean frequency (+ s.e.m.) of total SIV-specific T cell responses within the CD4+ and CD8+

memory T cell populations of the designated tissues (BM = bone marrow) obtained from necropsy of the same ten completely protected macaques (*left panel*). Spearman analysis shows the correlation between the mean frequencies of SIV-specific CD8^{+} T cells in each tissue with the log mean of cell-associated SIV RNA in a corresponding tissue (*right panel*).
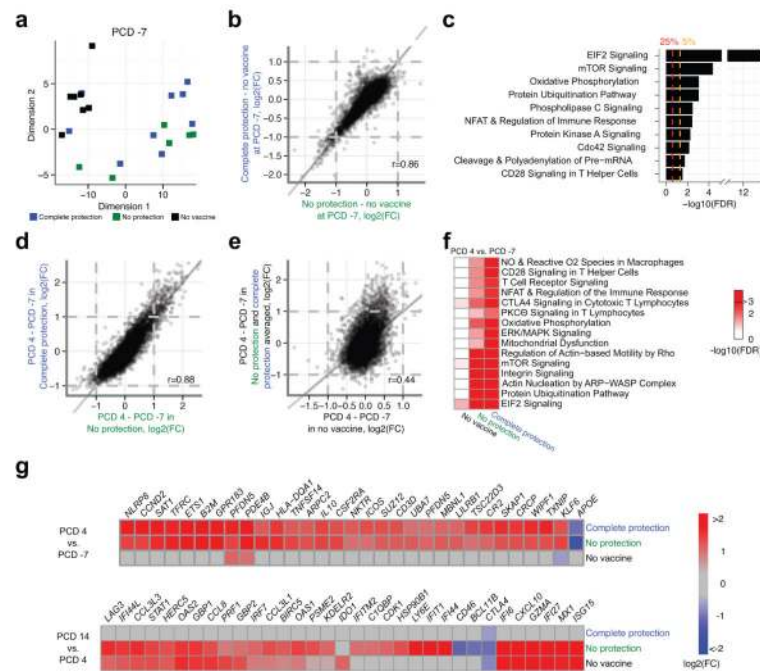
Figure 4. Transcriptional profiling of unfractionated lymph node cells before and after wildtype SIV challenge

(**a**) Comparison of overall gene expression profiles of pre-challenge (PCD -7) unfractionated lymph node cells from control (unvaccinated) macaques vs. LAV-vaccinated macaques that were either completely protected or non-protected after wildtype SIV challenge. Genes differentially expressed between these three groups were selected by F-test with a 5% false discovery rate (FDR), and then a multidimensional scaling method was used to visualize relatedness of the data sets (control vs. non-protected vs. completely protected macaques). (**b**) Scatterplot comparing gene expression levels between completely protected (*y-axis*) and non-protected (*x-axis*) macaques by fold-change (FC) relative to unvaccinated controls. Dashed lines indicate absolute 2-FC. (**c**) Top canonical pathways differentially expressed between vaccinated macaques (completely protected and non-protected groups averaged) and unvaccinated controls (C). Yellow and red dashed lines indicate thresholds for the pathway over-representation test FDR estimate of 5% and 25%, respectively. (**d**) Scatterplot comparing FC in gene expression from PCD -7 to PCD 4 in unfractionated lymph node cells between completely protected (*y-axis*) and non-protected (*x-axis*) macaques. (**e**) Scatterplot comparing FC in gene expression from PCD -7 to PCD 4 in unfractionated lymph node cells of unvaccinated controls (*x-axis*) to the average FC in the completely protected and non-protected macaques (*y-axis*). (**f**) Heat map of the top 15 differentially expressed canonical pathways by - $\log_{10}$(FDR) between PCD -7 and PCD 4 for control, non-protected and completely protected macaques (unvaccinated controls contributed no significant pathway > 5% FDR). (**g**) Heat map of average gene expression FC from PCD -7 to PCD 4 (upper) and PCD 4 to PCD 14 (lower) in unfractionated lymph node cells for control, non-protected and completely protected macaques. The genes shown in the heat map were selected by having absolute FC > 2 at 5% FDR in at least one protection outcome group and were immune-filtered (see Methods).
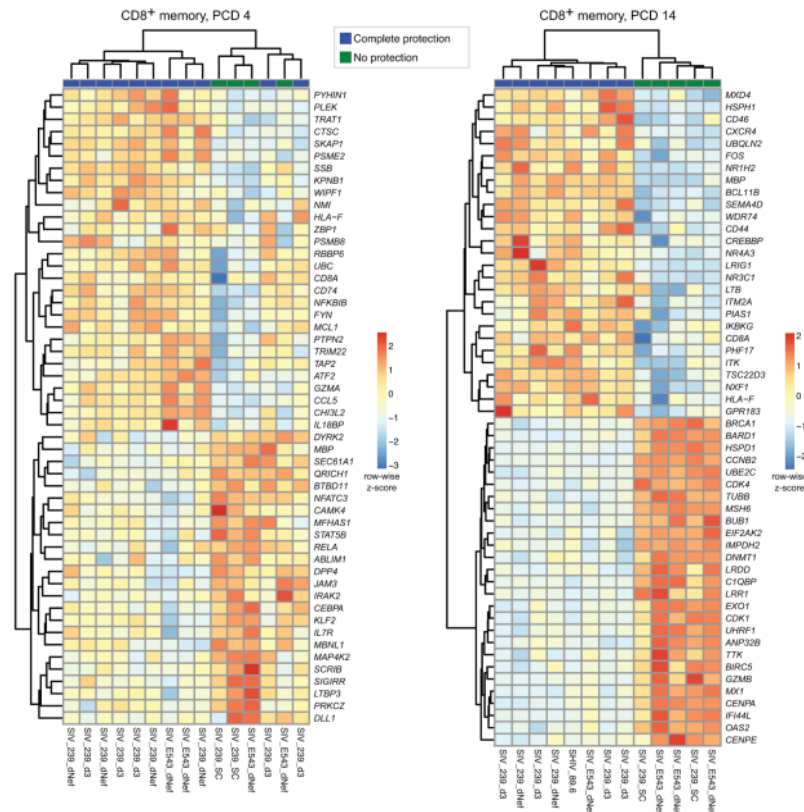
Figure 5. Transcriptional profiling of sorted lymph node CD8$^+$ T cells at day 4 and 14 after wildtype SIV challenge

CD8$^+$ memory T cells were isolated by cell sorting from lymph nodes taken 4 and 14 days post-challenge from non-protected and completely protected macaques for transcriptional analysis by microarray. The panels show heat map profiles of genes differentially expressed between lymph node CD8$^+$ memory T cells of completely protected vs. non-protected macaques at PCD 4 (left) and 14 (right). Immune-filtered gene expression is shown as gene-wise standardized expression (Z score), with absolute fold change > 1.3, *P* < 0.01 and false discovery rate < 25% chosen as the significance level.

Table 1

Kruskall-Wallis analysis of the 11 primary immune response predictors vs. the protection categories

Immune Predictors	Unadjusted *P* value	Bonferroni-corrected *P* value
PBMC CD4^{+} T cell response magnitude	0.0672	0.7392
PBMC CD8^{+} T cell response magnitude	0.0195	0.2148
PBMC CD4^{+} T cell response breadth	0.0301	0.3313
PBMC CD8^{+} T cell response breadth	0.1593	1.0000
Lymph node CD4^{+} T cell response magnitude	**0.0003**	**0.0036**
Lymph Node CD8^{+} T cell response magnitude	**0.0006**	**0.0070**
BAL CD4^{+} T cell response magnitude	0.0450	0.4950
BAL CD8^{+} T cell response magnitude	0.0221	0.2426
SIVmac239 neutralizing antibodies	0.1458	1.0000
SIVenv-specific antibodies; TCLA-SIVmac251 neutralization	0.0079	0.0872
SIVenv-specific antibodies; ADCC	0.0073	0.0808